Low-lying dipole response in the unstable ^{70}Ni nucleus

O. Wieland,[1,*] A. Bracco,[2,1] F. Camera,[2,1] R. Avigo,[2,1] H. Baba,[3] N. Nakatsuka,[4,3,5] T. Aumann,[5,6] S. R. Banerjee,[7] G. Benzoni,[1] K. Boretzky,[6] C. Caesar,[5,6] S. Ceruti,[2,1] S. Chen,[8,3] F. C. L. Crespi,[2,1] V. Derya,[9] P. Doornenbal,[3] N. Fukuda,[3] A. Giaz,[2,1] K. Ieki,[10] N. Kobayashi,[11] Y. Kondo,[12] S. Koyama,[11] T. Kubo,[3] M. Matsushita,[13] B. Million,[1] T. Motobayashi,[3] T. Nakamura,[12] M. Nishimura,[3] H. Otsu,[3] T. Ozaki,[12] A. T. Saito,[12] H. Sakurai,[11,3] H. Scheit,[5] F. Schindler,[5,6] P. Schrock,[5] Y. Shiga,[10,3] M. Shikata,[12] S. Shimoura,[13] D. Steppenbeck,[3] T. Sumikama,[3] S. Takeuchi,[3] R. Taniuchi,[11] Y. Togano,[12] J. Tscheuschner,[5] J. Tsubota,[12] H. Wang,[3] K. Wimmer,[11] and K. Yoneda[3]

[1]*INFN, Sezione di Milano, I-20133 Milano, Italy*
[2]*Dipartimento di Fisica dell'Università degli Studi di Milano, I-20133 Milano, Italy*
[3]*RIKEN Nishina Center, 2-1 Hirosawa, Wako, 351-0198 Saitama, Japan*
[4]*Department of Physics, Kyoto University, Kyoto 606-8502, Japan*
[5]*Institut für Kernphysik, Technische Universität Darmstadt, D-64289 Darmstadt, Germany*
[6]*GSI Helmholtzzentrum für Schwerionenforschung GmbH, D-64291 Darmstadt, Germany*
[7]*Variable Energy Cyclotron Centre, 1/AF-Bidhannagar, Kolkata-700064, India*
[8]*School of Physics and State Key Laboratory of Nuclear Physics and Technology, Peking University, Beijing 100871, China*
[9]*Institut für Kernphysik, Universität zu Köln, D-50937 Köln, Germany*
[10]*Department of Physics, Rikkyo University, Tokyo 171-8501, Japan*
[11]*Department of Physics, The University of Tokyo, Tokyo 113-0033, Japan*
[12]*Department of Physics, Tokyo Institute of Technology, Tokyo 152-8551, Japan*
[13]*Center for Nuclear Study, The University of Tokyo, Tokyo 113-0033, Japan*

(Received 1 August 2018; published 11 December 2018)

The Coulomb excitation of the neutron-rich nucleus ^{70}Ni was measured in inverse kinematics at 260A MeV bombarding energy and with a ^{197}Au target. The beam energy allowed us to study the dipole response around the neutron separation energy (up to about 12 MeV). The experiment was performed at the RIKEN Radioactive Isotope Beam Factory (RIBF). The γ decay from the scattered ^{70}Ni ions at around zero degree was measured with a scintillator detection system composed of large volume $LaBr_3$:Ce detectors (HECTOR$^+$ array) and NaI(Tl) detectors (DALI2 array). Results were obtained for the $E1$ strength in the region where the dipole response is characterized by the presence of the pygmy dipole resonance. The measured $E1$ strength is found to be larger as compared with that of ^{68}Ni below the neutron binding energy. The measured $E1$ strength as a function of energy is compared with available predictions based on relativistic and nonrelativistic approaches, and only in some cases does theory give a reasonable account of the data.

DOI: 10.1103/PhysRevC.98.064313

I. INTRODUCTION

The understanding of the electric response of dipole type, mainly due collective vibrational dipole mode [1], is needed because this mode provides one of the key basic pieces of information on nuclear properties. This information is particularly important in the uncharted region of nuclei far from stability where experimental studies are scarce. In the case of neutron-rich nuclei one relevant property of the dipole response is the presence of a strength exceeding that of the tail of the Lorentzian strength function giving the shape of the giant dipole resonance. This extra strength is called the "pygmy dipole resonance" and, in the case of stable nuclei, has been the subject of several studies (see e.g., the reviews [2–4]). For nuclei far from stability in the medium-mass region only the ^{68}Ni and ^{131,132,133}Sn nuclei were investigated. While for Sn isotopes the Coulomb neutron dissociation was measured [5], in the case of ^{68}Ni both the Coulomb neutron dissociation and the virtual photon-scattering methods were used [6–8]. The latter has the advantage of being able to probe the region below the neutron binding energy.

Far from stability, neutron-rich nuclei are important for learning about neutron matter properties because they provide very useful inputs for the nuclear equation of state, which is relevant [9,10] for modeling neutron stars [11,12] and their merging. The low-lying $E1$ strength has a connection to properties of the isovector part of the equation of state (EoS) of nuclear matter (see, e.g., Refs. [10,13,14]). This connection is found to be particularly strong via the dipole polarizability, which in turn can be linearly connected [15] to the neutron skin. The dipole polarizability is obtained as an integral over the excitation energy of the dipole cross section divided by the square of the excitation energy and, thus, depending on the value of its cross section, the pygmy region with only a few percent of the energy-weighted sum rule gives a sizable

*oliver.wieland@mi.infn.it

value to the polarizability (up to the order 20% and perhaps even more). It has to be pointed out that the connection of the nuclear polarizability and the neutron skin is model dependent, so that improvements in the theory are relevant for this purpose. The study of the pygmy states, described as excitation of the neutron skin, is thus important in order to give additional experimental constraints to theory [16]. Indeed a comprehensive test of microscopic models using multiple observables is a very useful approach to make more solid the application EoS in the study of neutron stars. Particularly interesting for this purpose is the investigation of the evolution of the pygmy strength in nuclei magic in proton numbers, as in the case of the Ni isotopes. It is interesting to determine whether the excitation of neutrons in the nuclear surface becomes more important with increasing neutron number [4].

It is also important to point out that the presence of $E1$ strength below the neutron binding energy plays a role on the evaluation of the size of reaction rates in calculations of the synthesis of the heavy elements [17] for astrophysical models in which unstable nuclei are involved. The strength in the pygmy region is directly linked to the radiative strength function, which is one of the main ingredients within the statistical model used in r-process description. The determination of the low-lying $E1$ strength in nuclei, particularly those far from stability, is therefore important for the reliability of such types of calculations. Therefore, also in this connection, an extensive test of the strength of the PDR in modern microscopic calculations is mandatory.

This paper addresses the study of the low-lying electric-dipole response in ^{70}Ni up to an excitation energy of 12 MeV. There are presently several theoretical works, also for this nucleus, employing different effective interactions that need to be tested. Moreover, in contrast with the previous works on the ^{68}Ni nucleus, this work on the ^{70}Ni isotope has better sensitivity in the region below the neutron separation energy S_n ($\approx$7.3 MeV) starting from around the $E > 4$ MeV region. This region of excitation energy, although of rather small size, is indeed interesting and has been the particular focus of the study of the PDR in stable nuclei. Here we study this region for in a nucleus in the medium-mass region far from stability by using the Coulomb excitation.

II. EXPERIMENT

The experiment [18] was performed at the RIBF facility of the RIKEN Nishina Center. A ^{238}U primary beam, at 345A MeV with an average intensity of 25 pnA, impinged on a rotating Be target (1 g/cm^2 thick). The secondary beam was produced via fission and had an incident energy of 260A MeV. By using the BigRIPS magnetic separator [19], the ^{70}Ni ions were selected and transported to a secondary Au target. The particle identification (PID) plot of BigRIPS obtained for this experiment is shown in the left panel in Fig. 1. The beam particle identification employed the TOF-$B\rho$-ΔE method, where TOF, $B\rho$, and ΔE are time of flight, magnetic rigidity, and energy loss, respectively. This allowed the identification of the atomic number Z and the mass-to-charge ratio A/Q for each ion. The intensity of the ^{70}Ni ions was 3×10^4 s^{-1} (40% of the total). The secondary target was made of gold and this choice

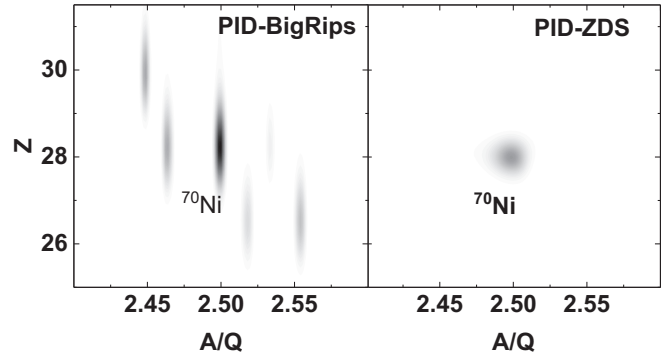

FIG. 1. Particle identification plots with the relation of Z and A/Q of the measured nuclei. The left panel identifies the secondary beam in front of the Au reaction target with BigRIPS spectrometer (see text). The right panel shows the distribution measured with the Zero Degree Spectrometer after the target (see text) and with ^{70}Ni isotopes selected in the incoming beam distribution.

is due to the high value of Z and to fact that this element is mono-isotopic. Moreover, when gold nuclei are excited, the emitted γ rays with the largest intensity; namely, those from the first-excited state, have energy less than that of the region of interest. Reaction products from the secondary target were identified by using the Zero Degree Spectrometer [19,20] in large acceptance mode [see PID Fig. 1 (right panel)]. The γ rays produced at the secondary target were detected with a setup including two arrays: one being DALI2 [21] and consisting of 96 NaI(TI) scintillators, mainly covering the central and backward angles, and the other array being HECTOR$^+$ and consisting of eight large-volume $LaBr_3$:Ce scintillator detectors [22] placed at forward angles. DALI2 was mainly used as a high-efficiency multiplicity filter, while HECTOR$^+$ was devoted to the γ-ray spectroscopy up to high energies (up to around 15 MeV in the reference frame of the emitting nucleus). The latter was placed at 44 cm from the target and in the forward direction at an angle of 30°. The intrinsic energy resolution (full width at half maximum, or FWHM) of $LaBr_3$:Ce was 1.60% at 6.31 MeV. The efficiency was 0.90% at 1.836 MeV (measured by using a ^{88}Y source), a value reproduced within 2.0% by a Monte Carlo simulation for this experiment obtained by using the code GEANT4 [23]. At higher energies the efficiency was measured with different radioactive sources and high-energy γ-ray beams [24]. The time resolution of the $LaBr_3$:Ce detectors was 1 ns (FWHM) for in-beam events, and this allowed us to reject a large fraction of background events. To select Coulomb excitation events, the condition of detecting scattered ^{70}Ni ions at 0° with an opening of 28 ± 5 mrad was applied. The nuclear contribution here amounts to 10(5)%. This value was deduced from measurements with ^{72}Ni and ^{74}Zn beams on a ^{12}C target [25], which were made at the same energy and by using similar detection conditions of this experiment. The measured nuclear reaction cross sections were finally validated by calculations based on the distorted wave Born approximation (DWBA) and coupled-channel (CC) approaches, which were performed by using the computer code ECIS [26]. For these calculations the optical potential employed was the one from Furumoto

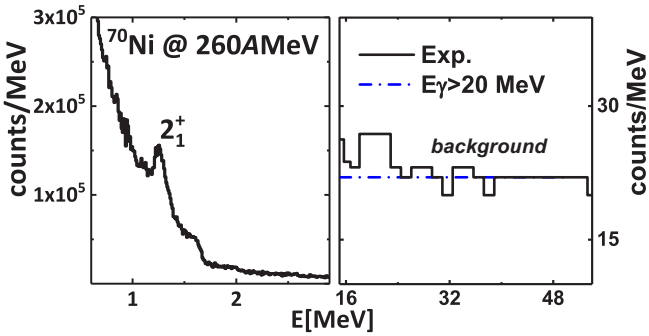

FIG. 2. The measured Doppler-corrected γ-ray spectrum in the two extreme regions measured in the experiment. The low-energy region in the left panel shows the excitation of the 2^+ state in ^{70}Ni. The high-energy region is shown in the right panel. The average counts in the region 20–50 MeV are assumed to be a background that was extrapolated to the region of interest (4–14 MeV) and then subtracted.

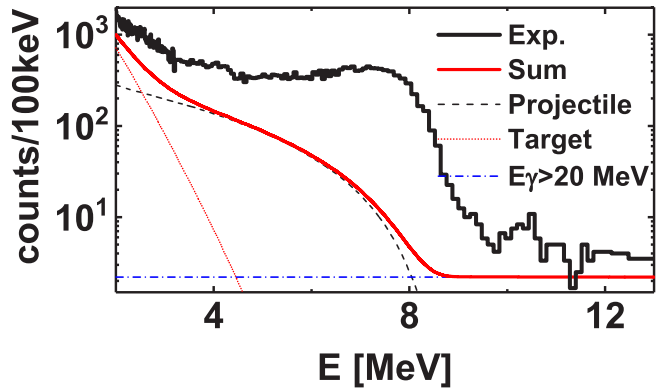

FIG. 3. Measured γ-ray spectrum (thick line) and simulations. The dotted and short dashed lines give the statistical decay of the target and projectile, respectively. The long dashed line is the extrapolation of the fit of counts above 20 MeV. The solid line is the sum of these contributions.

[27–29]. The angular position of the outgoing ^{70}Ni ions was measured event by event in order to correct for the Doppler effect. After Doppler reconstruction, the energy resolution of the $LaBr_3$:Ce detectors was, on average, 9%.

Figure 2 shows the measured γ-ray spectrum for ^{70}Ni in two different energy regions. The left panel displays the Doppler-corrected γ-ray spectrum up to 3 MeV and in the right panel are displayed the data above 15 MeV, the latter in bins 1.6 MeV wide. Note that the shape of the spectrum between 20 and 50 MeV is basically flat because of the lowering of the virtual photon flux and the very small γ-branching no signals from the giant dipole resonance (GDR) is expected, but only a few counts of background, mainly from cosmics. For the evaluation of this background the approach of taking a line extrapolated by a regression fit has been used, as shown in the right panel of Fig. 2. The peak in the left panel corresponds to the excitation of the known 2^+ state at 1.260 MeV. The population cross section and $B(E2)$ value of $428(\pm50)(\pm200)$ $e^2\,\mathrm{fm}^4$ for this excited state is found to be consistent within the error bars with the $B(E2)$ reported in Refs. [30,31]. The discussion of the measurement of the $B(E2)$ extracted with this experiment is the subject of another presentation since the theoretical models addressing this quantity differ from those existing for the $B(E1)$ at higher excitation energy.

The measured γ-ray spectrum for ^{70}Ni in the region 2–13 MeV is shown in Fig. 3. It was obtained by using the $LaBr_3$:Ce data requiring scattered ^{70}Ni ions and applying a narrow gate on the time of flight of the γ rays (±1 ns). To favor the detection of ground-state decays this spectrum was obtained by requesting multiplicity one for γ-ray emission. Because of the excitation mechanism, this spectrum at $E > 4$ MeV is expected to be dominated by $E1$ transitions. This is supported by the measurement of the ratio of the cross section in the region 5–8 MeV with that of the 2^+ state as a function of the angle of the detected γ rays. These data, shown in Fig. 4, are well reproduced by Eikonal predictions obtained with the computer code DWEIKO [32] which uses the distorted-wave approach. For these ratio calculations we assumed $E1$ decay in the region 5–8 MeV together with the known $E2$ decay at 1.26 MeV and normalized the datum at 30° (see the red curve in Fig. 4).

The measured spectrum of Fig. 3 contains direct decays but also decays from compound nuclei. The latter was computed with the statistical model [8,33] and considering the decay of the excited nuclei of the target and of the projectile (the dotted and short-dashed lines in Fig. 3, respectively). These calculations of the γ-ray emission were made by using the code GEMINI++ [34,35], which employs a Monte Carlo approach. The calculations of the γ-ray emission were done at each excitation-energy bin, starting from the population of states of 1^- type with a cross section decreasing as a

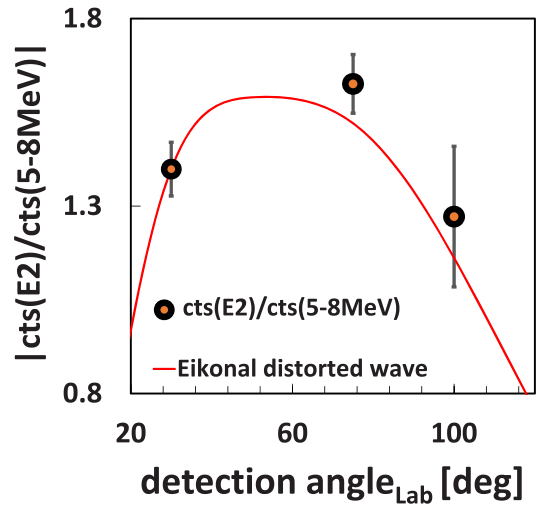

FIG. 4. The plot shows the ratio of the yield in the region 5 MeV $< E_\gamma <$ 8 MeV with that of the first 2^+ state as a function of the angle of the emitted γ rays. The corresponding distorted wave predictions (eikonal type) for this ratio assuming $E1$ and $E2$ decay is shown with a red curve.

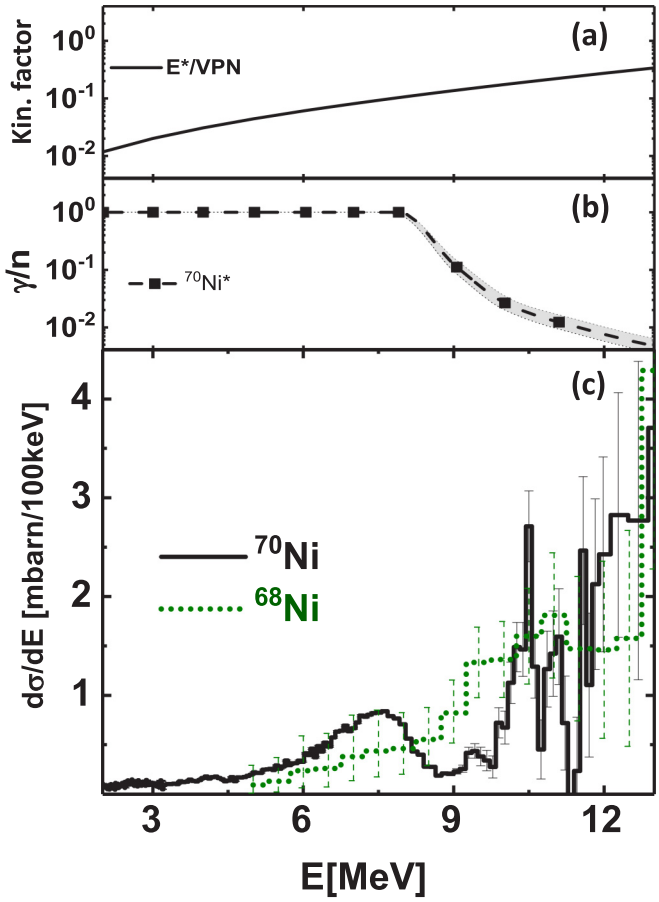

FIG. 5. (a) Quantities used to obtain the cross section in panel (c) and in Fig. 7 (lowest panel). The kinematical factor contains the virtual photon number (VPN) and energy of the photon. (b) The γ/n branching ratio. The shaded area shows the uncertainty [38] for the level density used in the statistical model. (c) The cross section for the Coulomb excitation of ^{70}Ni as a function of energy (full drawn line). The data for ^{68}Ni [8] are shown with a dotted green line.

function of excitation energy in the same way as that of the virtual photon spectrum (see top panel of Fig. 5, showing the kinematical factor containing the inverse of the virtual photon spectrum). This is also supported by the measurement of the angular distribution of the high energy gamma-rays. For the $E1$ strength a single Lorentzian centered at 18.02 MeV (13.73 MeV) and with a width of 6.73 MeV (4.74 MeV) was used for ^{70}Ni (^{197}Au). For the level density, an important quantity to deduce the gamma decay in competition to the neutron emission, the value from the RIPL3 database [36] was used. This level density was chosen since it is the one which is presently widely employed. In the next section the calculation of values of the γ/n branching ratio are described and shown in Fig. 5. Other important quantities considered for these calculations are the target thickness, the number of incident particles, the detector response function, and the Doppler correction. To mimic the experimental conditions which allow us to determine the velocity and angle of the emitting projectile nuclei only, the emission from the excited target nuclei was corrected by the Doppler of the projectile. This resulted in the emission spectrum from target nuclei to be decreasing very fast within 4 MeV. The computed sum spectrum obtained by adding the statistical model calculations (for the target and of the projectile) and the background (the continuous red line in Fig. 3 assumed to be due mainly to cosmics events and deduced from the counts in the interval 20–50 MeV) was subtracted from the measured spectrum and this resulted in the yield of interest discussed in the next section.

III. $E1$ STRENGTH

The measured γ-ray spectrum for ^{70}Ni in the region 3–13 MeV was used to obtain the electric-dipole strength for this nucleus. The experimental yield, after subtracting the contribution due to the statistical emission of the target and projectile was then converted into the excitation cross section. For this purpose the standard kinematical factor [in Fig. 5(a)] was used. The latter was deduced by using the method in Ref. [37] and assuming virtual photons of $E1$ type. In the region above 7.3 MeV (a value of S_n for ^{70}Ni) the γ/n branching ratio [in Fig. 5(b)] was taken into account to determine the excitation strength. Owing to the detection resolution, a measurable branching starts from 7.9 MeV. The γ/n branching ratio is a critical point in the analysis and is found to depend mainly on the level density, which is not always well pinned down experimentally.

The computation of the γ/n branching ratio is done within the statistical model by using the computer code GEMINI++ for calculating the decay cascades. The calculation of this branching requires as input three quantities: One is an assumption of the entry point taken as the population of states of 1^- type since at the virtual photon spectrum is dominated by $E1$ ones at angles at which the measurement is made. The second quantity is the neutron transmission coefficient, and for this we used the value tabulated in the GEMINI code, which was deduced by making use of neutron absorption cross sections and by using the principle of detailed balance. The third and most important quantity, on which this ratio has the strongest dependence, is the level density. In our case we used the level density given in the RIPL3 database [36], which is presently widely employed. Moreover, a recent measurement of the level density of $E1$ states in the region 6–20 MeV for the nucleus ^{96}Mo [38] was compared with three different calculated level densities and it was found that only the prediction from the RIPL3 database reproduces the data. For our analysis we then considered as uncertainty the experimental uncertainties of the work on ^{96}Mo [38]. This choice resulted in the shaded band areas in Figs. 5(b) and 6.

The Coulomb excitation cross section for ^{70}Ni as deduced from γ-ray emission events is shown in Fig. 5(c) in the region 2–13 MeV together with the data from the previous measurement for ^{68}Ni [8]. The measured spectral distribution for ^{70}Ni is characterized by two distinctive features: one is an increase of strength followed by a drop of counts at around 8 MeV due to the neutron emission threshold which reduces the γ-ray emission; the other is a general raising trend of the cross section above the neutron binding energy, although with fluctuations due to the low statistics of counts in the measured

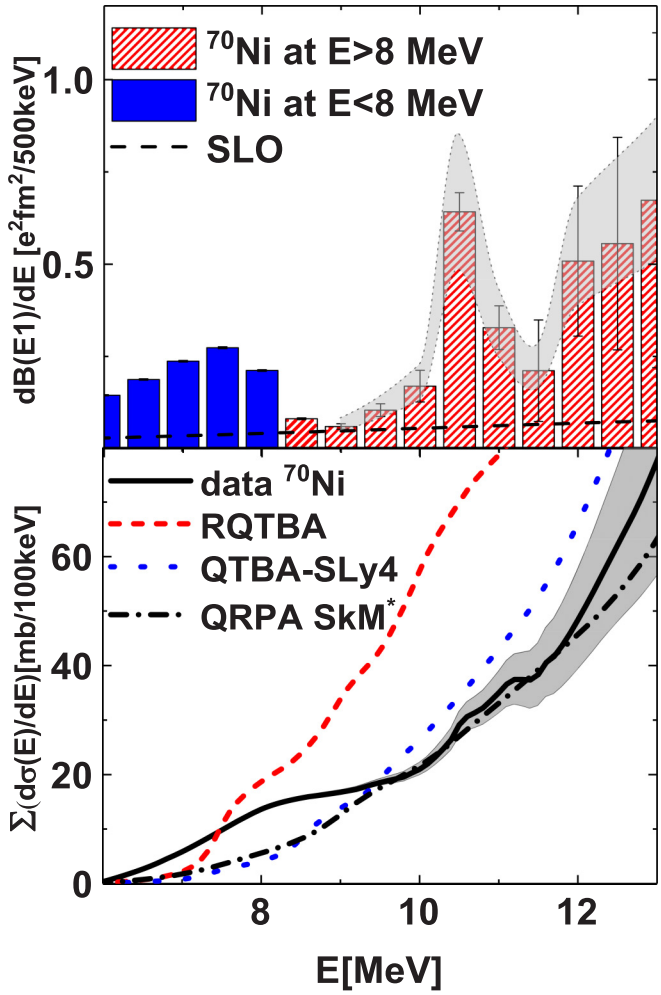

FIG. 6. The $E1$ strength extracted from the data of Fig. 7(d). The filled (dashed) bars are the data below (above) 8 MeV (being S_n = 7.3 MeV). The dashed line shows the standard Lorentzian (SLO) values [39] for the giant dipole resonance (GDR) with centroid $E_{GDR} = 18.2$ MeV and width $\Gamma_{GDR} = 6.7$ MeV as from the database [36]. The shaded area shows the confidence band of the $E1$ strength due to the uncertainty in the level density used in the statistical model calculations, which lies within the statistical errors bars. The lower panel shows the running sum of the experimental $E1$ cross section for ^{70}Ni with the full-drawn line and with the shaded area including errors. The same three different predictions as in the upper panel for ^{70}Ni are also shown for the running sum (see text and the legend).

spectrum. It is in general difficult to infer the shape of the $B(E1)$ at the binding energy because the modeling of the γ/n branching shows an abrupt behavior. This behavior could produce a type of an artifact for the $B(E1)$ slope at 8 MeV and therefore should be taken with caution. This is why, in the same figure, we give the value used for the γ/n branching to make the reader aware of it. With the available information we cannot do better but, on the other hand, by noticing that there is a rising of the $E1$ strength from 6 to 8 MeV one cannot exclude that this is a bump peaking at about 7.5 MeV. If one assumes the γ/n ratio to be smoother at around 8 MeV one obtains a slightly less sloping $E1$ spectrum corresponding to a change of 5% in the $B(E1)$ value. However, one can see that there is on average an increase of the cross section towards the centroid of the GDR expected to be at around 18 MeV [36]. By examining Fig. 5(c) one sees that improvements in efficiency and energy resolution are key factors for this type of studies. In addition, the comparison of the ^{70}Ni data with the ^{68}Ni data clearly shows that for the ^{70}Ni nucleus there is an additional strength at lower energy. A simple explanation, also justified by the existing systematics on stable nuclei, could be related to the increase in neutron number by going from ^{68}Ni to ^{70}Ni. Note that the experimental sensitivity to decays below neutron binding was much lower in the case of ^{68}Ni than in the present experiment.

The $E1$ strength corresponding to the measured cross section is shown with filled (dashed) bars below 8 MeV (above 8 MeV) in Fig. 6 (upper panel) as a function of energy. The difference in visualization is to recall the correction that was made by using the γ/n branching. The energy resolution of the detectors (varying between 0.9 to 1.8 MeV going from 6 to 12 MeV) does not allow us to identify fine structures in the strength function. The shaded area at energy $E >$ 8 MeV shows the deduced strength when the uncertainty in the γ/n branching is taken into account (as described above in connection with Fig. 5).

The deduced $E1$ strength and the fraction of the energy-weighted sum rule (EWSR) are $1.06 \pm 0.14\ e^2\,\mathrm{fm}^2$ ($1.5\% \pm 0.2\%$) at 6–8 MeV and $2.2 \pm 0.4\ e^2\,\mathrm{fm}^2$ ($4.8\% \pm 0.9\%$) at 8–12 MeV. One important uncertainty in the normalization is due to the presence of isomeric states in the beam. The isomeric content of the beam was measured with the same experimental setup and beam condition in another dedicated measurement [25]. The value of 6.9(9)% was found and thus a number of ions corresponding to this fraction was subtracted in the case for the determination of the first 2^+ state from the total measured ions to determine the cross section for prompt-γ-ray emission. In this way we are in the same conditions as those of the direct kinematic experiment where the nuclei in the target are in the ground state. Concerning the GDR built on the isomeric 8^+ state, this contribution is included (see, e.g., Ref. [40] presenting data with gates on isomeric states). The systematic error of the $B(E1)$ includes the correction due to the feeding of high-energy γ rays into the first-excited state. For this purpose, γ-γ coincidences were used. The total number of high-energy γ rays (with $E_\gamma > 4$ MeV) in coincidence with the first-excited states corrected for efficiency divided by the number of single events provided the feeding. It was found to be 8(2)%. One can note a significant excess of strength around S_n as compared with the simplest prediction [dashed line in Fig. 6 (upper panel)] based on a single Lorentzian function (SLO) for GDR [36,39] not including a pygmy strength.

Several predictions are available for the $E1$ response in ^{70}Ni which use different approaches in terms of the involved nuclear configurations and interaction types [41–47]. It is interesting to compare them to the present result by using the running sum quantity. Figure 6 (lower panel) shows this comparison between experimental ^{70}Ni data (full-drawn line) and predictions including a shaded area of the experimental uncertainty around the data. The different predictions are

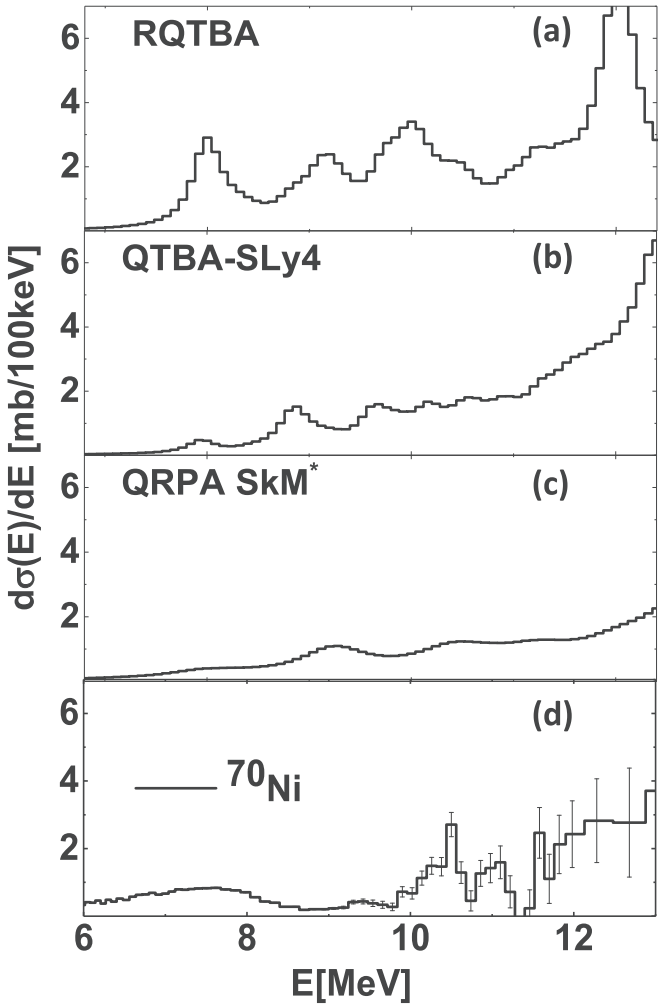

FIG. 7. Comparison of theoretical calculations of the $E1$ cross section distribution with the experiment. (a)–(c) The predicted $E1$ cross section for ^{70}Ni is shown for three different predictions for ^{70}Ni (see text). (d) The measured cross section for the Coulomb excitation of ^{70}Ni as a function of energy.

(i) calculations made with the quasiparticle random-phase approximation (QRPA) method and using as interaction the Skyrme interaction denoted SkM* [41,42] [Fig. 7(c) and dotted-dashed line in Fig. 6 (lower panel)]; (ii) calculations made with the quasiparticle time-blocking approximation (QTBA) method and using the interaction the Skyrme force denoted SLy4 [43,44,48] [Fig. 7(b) and dotted line in Fig. 6 (lower panel)] and (iii) calculations made with the relativistic quasiparticle time-blocking approximation (RQTBA) method and using the interaction denoted NL3 [45–47] [Fig. 7(a) and dashed line in Fig. 6 (lower panel)]. From the comparison of the data with predictions one finds agreement for the QRPA and QTBA calculations but only in the region $E > 9$ MeV. Both calculations are based on two different Skyrme effective interactions and many-body techniques. The first is based on the small amplitude of a time-dependent Hartree–Fock (HF) calculation, the second includes important contributions beyond the HF approach. In contrast, the RQTBA calculation, allowing a parameter-free description of the fragmentation of the 1^- states induced by coupling to phonons, gives a satisfactory agreement with the data at low energy but fails above 8 MeV, resulting in an excess of strength. To see more details of these calculations one should examine Fig. 7 which shows the energy distribution of the cross section in the region of interest in comparison with the data. Also in this case it is difficult to select the theory which better reproduces the data, although there is a common feature for the three predictions, that of having strength also below the neutron binding energy. It is clear that the predictions depend on the many-body approach used (see also, e.g., Ref. [13] for ^{68}Ni) and further effort, concentrating on the low-energy part, should be made to improve the description of the data.

IV. CONCLUSION

This work has provided for the first time a measurement of 1^- PDR states in ^{70}Ni by using the Coulomb excitation process populating selectively these states. The $E1$ strength, measured in the unstable nucleus in the region below and above particle binding energy, suggests some softening of the pygmy strength for ^{70}Ni. In addition, the comparison of the ^{68}Ni [8] and ^{70}Ni data, in particular if integrated in the region 6–8 MeV, shows an increase with neutron number. This integrated strength is 0.6 ± 0.22 e^2 fm^2 for ^{68}Ni and 1.06 ± 0.14 e^2 fm^2 for ^{70}Ni. However, it should be pointed out that the experimental conditions for the ^{68}Ni data were less ideal to probe that region and thus measurements with better sensitivity are called also for this nucleus. At this level the presence of additional undetected strength in ^{68}Ni below neutron binding cannot be excluded. To be pointed out that a very recent work on the γ strength function of ^{70}Ni provided also some evidence of a pygmy strength below the binding energy. In that work the experimental approach is different and the signal for the PDR is related to the presence of an upbend in the γ strength function [49]. In addition, the beta-decay approach used in that interesting paper is probing only particular decay paths [50].

For the $E1$ strength the comparison between data and theory is satisfactory above 9 MeV for predictions obtained with the QRPA and QTBA methods (with the SkM and SLy4 interactions). At $E < 9$ MeV the predictions obtained with the RQTBA method (and NL3 interaction) which include phonon couplings give a better account of the data. Improved calculations require refined modeling which is needed to provide a better interpretation of the experimental data [17,51–53].

It should be pointed out that efforts are presently being made to perform fully microscopic calculations (e.g., the advanced large-scale interacting shell-model calculations [54]) to predict the fragmentation of the dipole and quadrupole strengths around the binding energy. These calculations need quite extensive computational power and are still under development in this mass region for 1^- states at low-medium energy [55,56].

Further studies are needed for the more neutron rich Ni isotopes to see whether there is a further softening of the pygmy states and to learn more on the nature of these 1^- states, such as their isovector and isoscalar components. For this last point one needs to use also other probes (see, e.g., Refs. [57–60]).

Recent results on unstable nuclei using as a target nuclei ^{4}He and ^{12}C were obtained for ^{20}O and ^{68}Ni beams showing the expected presence of an isoscalar component in the pygmy region. In light nuclei, however, single-particle states play a role in the $E1$ response.

Another mass region of great interest, presently under investigation with new measurements, is that of neutron-rich Ca isotopes. There, predictions using complex computations based on the shell model are available [54,55,61] for low-lying states and masses and tested in experiments [62,63].

The most difficult experimental effort for the future is the improvement of the energy resolution of the γ-ray detection which is a key issue to determine the fine structures that, based on systematic studies in stable nuclei, are expected to be present. The fine structure gives more insight into the nature of these states. This improvement requires the employment of γ-tracking techniques as in the arrays AGATA and GRETA.

Moreover, this work calls for further development of a theoretical framework describing the pygmy 1^- states below neutron and around the particle binding energy. For example, one direction could be a better modeling of the phonon vibration couplings which are at play in general in many-body systems and are known to provide the width of the giant dipole resonance.

ACKNOWLEDGMENTS

We thank the RIKEN accelerator team for supplying the beam, T. Furumoto for discussions and providing the nuclear potential, E. Litvinova, O.I. Achakovskiy, S.P. Kamerdzhiev, X. Roca–Maza, and Y.F. Niu for discussions and theoretical calculations of the 1^- states. This work was partly supported by JSPS Kakenhi Grant No. 16H02179, and MEXT Kakenhi Grant No. 24105005 in Japan and by INFN Italy.

[1] M. N. Harakeh and A. van der Woude, *Giant Resonances* (Clarendon Press, Oxford, 2002).
[2] B. Abbott *et al.*, Astrophys. J. Lett. **848**, L12 (2017).
[3] A. Bracco *et al.*, Eur. Phys. J. A **51**, 99 (2015).
[4] D. Savran *et al.*, Prog. Part. Nucl. Phys. **70**, 210 (2013).
[5] P. Adrich, A. Klimkiewicz, M. Fallot, K. Boretzky, T. Aumann, D. Cortina-Gil, U. Datta Pramanik, T. W. Elze, H. Emling, H. Geissel, M. Hellström, K. L. Jones, J. V. Kratz, R. Kulessa, Y. Leifels, C. Nociforo, R. Palit, H. Simon, G. Surówka, K. Sümmerer, and W. Waluś (LAND-FRS Collaboration), Phys. Rev. Lett. **95**, 132501 (2005).
[6] D. M. Rossi, P. Adrich, F. Aksouh, H. Alvarez-Pol, T. Aumann, J. Benlliure, M. Böhmer, K. Boretzky, E. Casarejos, M. Chartier, A. Chatillon, D. Cortina-Gil, U. Datta Pramanik, H. Emling, O. Ershova, B. Fernandez-Dominguez, H. Geissel, M. Gorska, M. Heil, H. T. Johansson, A. Junghans, A. Kelic-Heil, O. Kiselev, A. Klimkiewicz, J. V. Kratz, R. Krücken, N. Kurz, M. Labiche, T. LeBleis, R. Lemmon, Y. A. Litvinov, K. Mahata, P. Maierbeck, A. Movsesyan, T. Nilsson, C. Nociforo, R. Palit, S. Paschalis, R. Plag, R. Reifarth, D. Savran, H. Scheit, H. Simon, K. Sümmerer, A. Wagner, W. Waluś, H. Weick, and M. Winkler, Phys. Rev. Lett. **111**, 242503 (2013).
[7] T. Aumann and T. Nakamura, Phys. Scr. **2013**, 014012 (2013).
[8] O. Wieland *et al.*, Phys. Rev. Lett. **102**, 092502 (2009).
[9] X. Roca-Maza and N. Paar, Prog. Part. Nucl. Phys. **101**, 96 (2018).
[10] N. Paar, C. C. Moustakidis, T. Marketin, D. Vretenar, and G. A. Lalazissis, Phys. Rev. C **90**, 011304(R) (2014).
[11] J. Piekarewicz, J. Phys.: Conf. Ser. **420**, 012143 (2013).
[12] J. Piekarewicz, J. Phys.: Conf. Ser. **492**, 012008 (2014).
[13] A. Carbone, G. Colo, A. Bracco, L. G. Cao, P. F. Bortignon, F. Camera, and O. Wieland, Phys. Rev. C **81**, 041301(R) (2010).
[14] X. Roca-Maza, M. Centelles, X. Vinas, and M. Warda, Phys. Rev. Lett. **106**, 252501 (2011).
[15] X. Roca-Maza, X. Vinas, M. Centelles, B. K. Agrawal, G. Colo, N. Paar, J. Piekarewicz, and D. Vretenar, Phys. Rev. C **92**, 064304 (2015).
[16] A. Klimkiewicz, N. Paar, P. Adrich, M. Fallot, K. Boretzky, T. Aumann, D. Cortina-Gil, U. Datta Pramanik, T. W. Elze, H. Emling, H. Geissel, M. Hellström, K. L. Jones, J. V. Kratz, R. Kulessa, C. Nociforo, R. Palit, H. Simon, G. Surówka, K. Sümmerer, D. Vretenar, and W. Waluś, Phys. Rev. C **76**, 051603(R) (2007).
[17] S. Goriely *et al.*, Nucl. Phys. A **739**, 331 (2004).
[18] R. Avigo *et al.*, RIKEN Accel. Prog. Rep. **48**, 41 (2015).
[19] T. Kubo *et al.*, Prog. Theor. Exp. Phys. **2012**, 03C003 (2012).
[20] N. Fukuda *et al.*, Nucl. Instrum. Methods Phys. Res., Sect. B **317**, 323 (2013).
[21] S. Takeuchi *et al.*, Nucl. Instrum. Methods Phys. Res., Sect. A **736**, 596 (2014).
[22] A. Giaz *et al.*, Nucl. Instrum. Methods Phys. Res., Sect. A **729**, 910 (2013).
[23] S. Agostinelli *et al.*, Nucl. Instrum. Methods Phys. Res., Sect. A **506**, 250 (2003).
[24] G. Gosta *et al.*, Nucl. Instrum. Methods Phys. Res., Sect. A **879**, 92 (2018).
[25] V. Modamio *et al.* (private communication; to be published).
[26] J. Raynal, Phys. Rev. C **23**, 2571 (1981).
[27] K. Li, Y. Ye, T. Motobayashi, H. Scheit, P. Doornenbal, S. Takeuchi, N. Aoi, M. Matsushita, E. Takeshita, D. Pang, and H. Sakurai, Phys. Rev. C **92**, 014608 (2015).
[28] T. Furumoto, W. Horiuchi, M. Takashina, Y. Yamamoto, and Y. Sakuragi, Phys. Rev. C **85**, 044607 (2012).
[29] T. Furumoto, Y. Sakuragi, and Y. Yamamoto, Phys. Rev. C **80**, 044614 (2009).
[30] O. Perru, O. Sorlin, S. Franchoo, F. Azaiez, E. Bouchez, C. Bourgeois, A. Chatillon, J. M. Daugas, Z. Dlouhy, Z. Dombrádi, C. Donzaud, L. Gaudefroy, H. Grawe, S. Grévy, D. Guillemaud-Mueller, F. Hammache, F. Ibrahim, Y. LeCoz, S. M. Lukyanov, I. Matea, J. Mrazek, F. Nowacki, Y. E. Penionzhkevich, F. de Oliveira Santos, F. Pougheon, M. G. Saint-Laurent, G. Sletten, M. Stanoiu, C. Stodel, C. Theisen, and D. Verney, Phys. Rev. Lett. **96**, 232501 (2006).
[31] K. Kolos, D. Miller, R. Grzywacz, H. Iwasaki, M. Al-Shudifat, D. Bazin, C. R. Bingham, T. Braunroth, G. Cerizza, A. Gade, A. Lemasson, S. N. Liddick, M. Madurga, C. Morse, M. Portillo, M. M. Rajabali, F. Recchia, L. L. Riedinger, P. Voss,

W. B. Walters, D. Weisshaar, K. Whitmore, K. Wimmer, and J. A. Tostevin, Phys. Rev. Lett. **116**, 122502 (2016).
[32] C. Bertulani, Comput. Phys. Commun. **116**, 345 (1999).
[33] J. Ritman, F. D. Berg, W. Kuhn, V. Metag, R. Novotny, M. Notheisen, P. Paul, M. Pfeiffer, O. Schwalb, H. Lohner, L. Venema, A. Gobbi, N. Herrmann, K. D. Hildenbrand, J. Mosner, R. S. Simon, K. Teh, J. P. Wessels, and T. Wienold, Phys. Rev. Lett. **70**, 533 (1993).
[34] R. Charity, Phys. Rev. C **82**, 014610 (2010).
[35] M. Ciemala *et al.*, Acta Phys. Pol., B **44**, 611 (2013).
[36] R. Capote *et al.*, Nucl. Data Sheets **110**, 3107 (2009).
[37] A. Winther and K. Alder, Nucl. Phys. A **319**, 518 (1979).
[38] D. Martin, P. von Neumann-Cosel, A. Tamii, N. Aoi, S. Bassauer, C. A. Bertulani, J. Carter, L. Donaldson, H. Fujita, Y. Fujita, T. Hashimoto, K. Hatanaka, T. Ito, A. Krugmann, B. Liu, Y. Maeda, K. Miki, R. Neveling, N. Pietralla, I. Poltoratska, V. Y. Ponomarev, A. Richter, T. Shima, T. Yamamoto, and M. Zweidinger, Phys. Rev. Lett. **119**, 182503 (2017).
[39] P. Axel, Phys. Rev. **126**, 671 (1962).
[40] M. Kmiecik, A. Maj, B. Million, M. Brekiesz, W. Królas, W. Meczyński, J. Styczen, M. Zięblíński, A. Bracco, F. Camera, G. Benzoni, S. Leoni, O. Wieland, S. Brambilla, B. Herskind, M. Kicińska-Habior, N. Dubray, J. Dudek, and N. Schunck, Phys. Rev. C **70**, 064317 (2004).
[41] X. Roca-Maza *et al.*, J. Phys. G **44**, 044001 (2017).
[42] Y. F. Niu, G. Colo, E. Vigezzi, C. L. Bai, and H. Sagawa, Phys. Rev. C **94**, 064328 (2016).
[43] O. Achakovskiy, A. Avdeenkov, S. Goriely, S. Kamerdzhiev, and S. Krewald, Phys. Rev. C **91**, 034620 (2015).
[44] O. Achakovskiya *et al.*, JETP Lett. **104**, 374 (2016).
[45] E. Litvinova, P. Ring, and V. Tselyaev, Phys. Rev. Lett. **105**, 022502 (2010).
[46] E. Litvinova, P. Ring, and V. Tselyaev, Phys. Rev. C **88**, 044320 (2013).
[47] G. A. Lalazissis, J. Konig, and P. Ring, Phys. Rev. C **55**, 540 (1997).
[48] E. Chabanat *et al.*, Nucl. Phys. A **635**, 231 (1998).
[49] A. C. Larsen, J. E. Midtbø, M. Guttormsen, T. Renstrøm, S. N. Liddick, A. Spyrou, S. Karampagia, B. A. Brown, O. Achakovskiy, S. Kamerdzhiev, D. L. Bleuel, A. Couture, L. C. Campo, B. P. Crider, A. C. Dombos, R. Lewis, S. Mosby, F. Naqvi, G. Perdikakis, C. J. Prokop, S. J. Quinn, and S. Siem, Phys. Rev. C **97**, 054329 (2018).
[50] M. Scheck, S. Mishev, V. Y. Ponomarev, R. Chapman, L. P. Gaffney, E. T. Gregor, N. Pietralla, P. Spagnoletti, D. Savran, and G. S. Simpson, Phys. Rev. Lett. **116**, 132501 (2016).
[51] E. Litvinova, P. Ring, V. Tselyaev, and K. Langanke, Phys. Rev. C **79**, 054312 (2009).
[52] I. Daoutidis and S. Goriely, Phys. Rev. C **86**, 034328 (2012).
[53] A. Tonchev *et al.*, Phys. Lett. B **772**, 20 (2017).
[54] Y. Tsunoda, T. Otsuka, N. Shimizu, M. Honma, and Y. Utsuno, Phys. Rev. C **89**, 031301(R) (2014).
[55] N. Shimizu *et al.*, Prog. Theor. Exp. Phys. **2012**, 01A205 (2012).
[56] T. Otsuka (private communication).
[57] N. Nakatsuka *et al.*, Phys. Lett. B **768**, 387 (2017).
[58] F. C. L. Crespi *et al.*, Phys. Rev. Lett. **113**, 012501 (2014).
[59] L. Pellegri *et al.*, Phys. Lett. B **738**, 519 (2014).
[60] D. Savran, M. Babilon, A. M. van den Berg, M. N. Harakeh, J. Hasper, A. Matic, H. J. Wörtche, and A. Zilges, Phys. Rev. Lett. **97**, 172502 (2006).
[61] N. Shimizu *et al.*, JPS Conf. Proc. **6**, 010021 (2015).
[62] R. G. Ruiz *et al.*, Nat. Phys. **12**, 594 (2016).
[63] D. Steppenbeck *et al.*, Nature (London) **502**, 207 (2013).